JOURNAL OF MATERIALS SCIENCE 13 (1978) 189–194

Stress corrosion characteristics of toughened glasses and ceramics

J. T. HAGAN, M. V. SWAIN, J. E. FIELD,
P.C.S., Cavendish Laboratory, Madingley Road, Cambridge, UK

A method for evaluating stress corrosion characteristics of thermally or chemically toughened glasses and ceramics is outlined. Values of the stress corrosion index n ($V = AK^n$) have been obtained and these are in excellent agreement with values for untreated materials. The analysis also explains the slightly greater absolute strength degradation observed for toughened glasses and ceramics.

1. Introduction

The extensive use of glasses and ceramics is limited by the relative weakness of these materials in tension. Their full potential is approached, however, by the application of various toughening techniques, whereby high compressive stresses are induced chemically or thermally in the surface regions of these materials. These biaxial compressive stresses have to be overcome before fracture occurs.

It has been shown by Kirchner and Walker [1] that the stress corrosion characteristics of toughened and untoughened alumina are the same and that the effect of the toughening is to provide sufficient strength at stress levels where failure usually occurs in untreated samples. Hagan and Swain [2] have made similar observations on chemically toughened calcium alumino silicate.

Attempts at using data from time to failure under static load or unnotched dynamic fatigue tests give anomalously high values of the stress corrosion index n for the toughened materials. Clearly the fracture stresses have to be corrected for the residual compressive stresses induced by the toughening. It is also apparent that the high tensile stresses in the middle of the toughened glasses or ceramics will have a significant effect on the times to failure, especially at stress levels not high enough to cause immediate failure. The analysis given here rationalizes the proper corrections to be applied to the stresses and the effect of the high tensile stress, in the central region, arising from the toughening.

To ensure equilibrium of forces throughout these toughened glasses and ceramics, the surface compressive stresses are balanced by internal tensile stresses. These internal stresses make it possible to determine the stable sub-critical crack growth rates using "macroscopic" cracks, as in, for example, the double torsion method. It is, however, still possible to obtain the stress corrosion characteristics from the time to failure or dynamic fatigue data; methods suggested by Evans and Johnson [3] for untoughened materials. The analysis presented here for toughened solids is an extension of their treatment.

2. Analysis

2.1. Residual tempering stresses

For both physically and chemically toughened glasses, the requirement for equilibrium is that the summation of the forces through the thickness, d, of the material must be zero;

$$\int_0^d \sigma(x)\,dx = 0 \qquad (1)$$

For thermally toughened glasses, the stress distribution throughout the thickness is parabolic (Zijlstra and Burggraaf [4]). Thus if the maximum compressive stress on the outer surfaces ($x = 0$, and $x = d$) is $-\sigma_c$, the parabolic stress distribution

is of the form

$$\sigma_t = \sigma_c(Ax^2 + Bx - 1) \tag{2}$$

where A and B are constants.

Consideration of Equation 1 and the boundary conditions, reduces Equation 2 to

$$\sigma_t = -\sigma_c\left(1 - \frac{6x}{d} + \frac{6x^2}{d^2}\right) \tag{3}$$

where the compression zone on either surface is ~20% of the plate thickness, and the maximum central tensile stress at $x = d/2$ is $\sigma_c/2$ as suggested by Zijlstra and Burggraaf [4]. The residual stress distribution is shown in Fig. 1a.

In the case of chemically toughened materials, the higher compressive stresses in the narrow surface layers are compensated for by a rather low and nearly constant tensile stress level over a large central region. The size of the compressive zone, δ, is determined by the fabrication process. Within this narrow compressive zone, the stress distribution is approximately linear as observed by Varshneya and Petti [5]. According to Lawn and Marshall [6], the stress distribution through the thickness is given by

$$\sigma_{c_t} = -\sigma_c\left(1 - \frac{x}{\delta}\right) 0 \leqslant x \leqslant \delta \tag{4a}$$

$$\sigma_{c_t} = -\sigma_c\left(1 - \frac{d}{\delta} + \frac{x}{\delta}\right) d - \delta \leqslant x \leqslant d \tag{4b}$$

for the stresses in the compressive zones, and

$$\sigma_{c_t} = \sigma_c(\delta/d) \tag{4c}$$

for the central zone, where δ is the characteristic

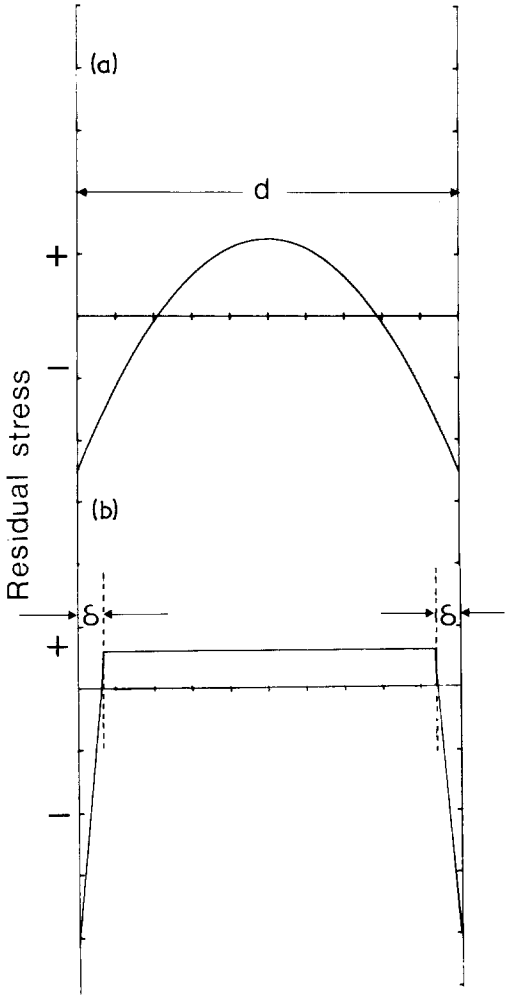

Figure 1 Residual stress distribution in (a) thermally and (b) chemically, toughened glasses and ceramics of thickness d units.

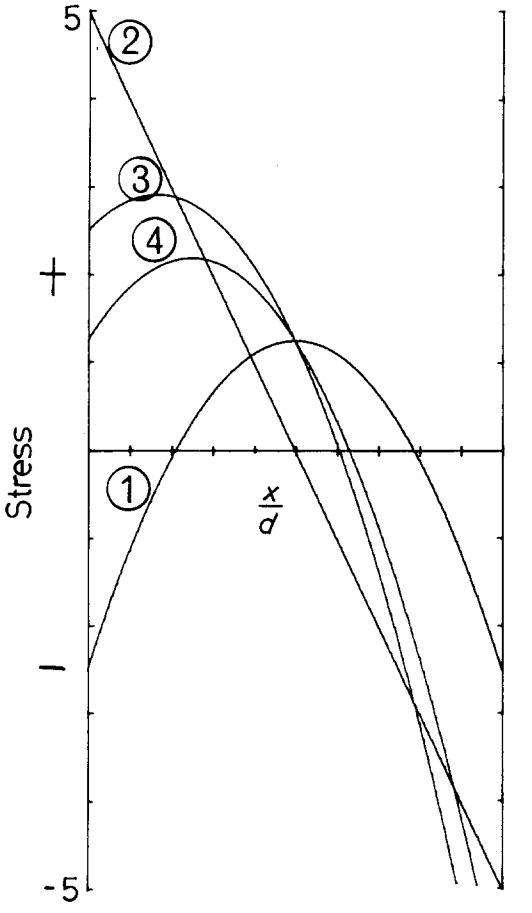

Figure 2 Stress distribution in plate. Curves 1 and 2 are the residual stress σ_c and bending stress σ_β^* respectively ($\sigma_\beta^* = 2\sigma_c$). The resultant of these is Curve 3. Curve 4 is the resultant stress for $\sigma_\beta^* = 1.5\,\sigma_c$ ($\sigma_c = 2.5$ units).

toughening depth and d is the specimen thickness. The stress profile through the thickness of the glass arising for chemically toughened materials is illustrated in Fig. 1b.

The treatment given here is for thermally toughened glasses and ceramics, but the analysis is essentially the same for chemically toughened materials if the proper stresses are used.

The stress distribution in a bar arising from flexure (four point bend test) is of the form

$$\sigma_\beta = \sigma_\beta^* \left(1 - \frac{2x}{d}\right) \tag{5}$$

where σ_β^* is the stress in the outer fibre (at $x = 0$). The resultant stress distribution (residual toughening stress and bending stress) is

$$\sigma = \sigma_t + \sigma_\beta \tag{6}$$

Substituting for σ_t and σ_β from Equations 3 and 5 respectively leads to

$$\sigma = (\sigma_\beta^* - \sigma_c) + \frac{x}{d}(6\sigma_c - 2\sigma_\beta^*) - \left(\frac{x}{d}\right)^2 6\sigma_c \tag{7}$$

This resultant stress σ for various values of σ_β^*/σ_c is shown in Fig. 2.

2.2. Stress intensity factor

For a straight, through-the-thickness crack, of infinite extent (with its origin at $x = 0$, and tip at $x = c$) in a single variable stress field of the form $\sigma = \sigma(x)$, the stress intensity factor, as given by Paris and Sih [7], is

$$K = 2Y\left(\frac{c}{\pi}\right)^{1/2} \int_0^c \frac{\sigma(x)\,dx}{\sqrt{c^2 - x^2}} \tag{8}$$

where Y is a dimensionless factor dependent on the crack shape, c the final crack length and $\sigma(x)$ is the stress function normal to the crack path. Equation 8 holds for internal cracks in infinite solids.

In the stress field defined by Equation 7 the stress intensity factor is given by

$$K = Y(\sigma_\beta^* - \sigma_c)(\pi c)^{1/2}\left[1 + \frac{\alpha c}{d}\right] \tag{9}$$

where

$$\alpha = \frac{2}{\pi}\left[\frac{6\sigma_c - 2\sigma_\beta^*}{\sigma_\beta^* - \sigma_c}\right]$$

and higher order terms are neglected. This equation only applies for a crack in an infinite solid.

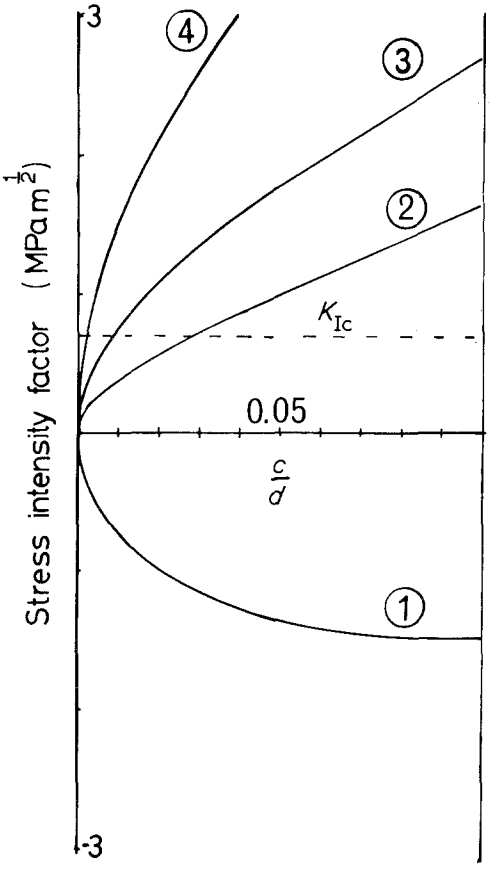

Figure 3 Stress intensity factor at crack tip in plate 5 mm thick for the ratios of applied stress σ_β^* to residual stress σ_c of $\sigma_\beta^*/\sigma_c = 0$, (Curve 1) 1.5 (curve 2), 2 (curve 3), 3 (curve 4). $\sigma_c = 60$ MPa. Dotted line is the position of K_{Ic} for soda lime glass.

For values of $c \ll d$ ($c < 0.1d$), this is a good approximation to the stress intensity factor for a semi-infinite solid in pure bending given by Brown and Srawley [8]. For larger values of c/d, a complete analysis needs to incorporate the interaction with the opposite boundary. Assuming a value of 60 MPa for the residual stress in a plate 5 mm thick and $Y = 1$, the stress intensity factors for 4 different values $\sigma_\beta^* = 0$, $1.5\,\sigma_c$, $2\,\sigma_c$ and $3\,\sigma_c$ are plotted in Fig. 3.

3. Time to failure under constant load

Knowing the stress intensity factor at the crack and a relationship between the crack velocity and the stress intensity factor driving the crack, one can obtain estimates of time of failure of components under the prescribed static stress. Since the basic difference between the toughened and untoughened material is the purely physical

residual stresses in the former, the stress corrosion characteristics should be the same for the two cases. Where the toughening is chemical, compositional changes may give rise to differences in the corrosion characteristics. For most materials, it has been shown to be a good approximation that the velocity and the stress intensity factor are related through

$$V = AK^n \tag{10}$$

where A and n are constants dependent on the material and the environment in which propagation occurs. The time to failure of the material under stress is

$$\tau = \int_{c_i}^{c_f} \frac{dc}{V} \tag{11a}$$

or

$$\tau = \int_{c_i}^{c_f} \frac{dc}{AK^n} \tag{11b}$$

where c_i and c_f are the initial and final crack lengths respectively.

Substituting for the stress intensity given by Equation 9 into 11b and assuming $Y = 1$, the time to failure becomes

$$\tau = \int_{c_i}^{c_f} \frac{dc}{A(\sigma_\beta^* - \sigma_c)^n (\pi)^{n/2} c^{n/2} \left[1 + \frac{\alpha c}{d}\right]^n} \tag{12}$$

Since $c/d < 0.1$, Equation 12 reduces to

$$\tau = \int_{c_2}^{c_1} \frac{dc}{A(\sigma_\beta^* - \sigma_c)^n (\pi)^{n/2}} c^{-n/2} \left[1 - \frac{n\alpha c}{d} + \ldots - \frac{n(n+1)(n+2)(n+3)(n+4)(n+5)}{6!} \alpha^6 \left(\frac{c}{d}\right)^6\right] \tag{13}$$

after taking the first 7 terms of the binomial expansion of $(1 + \alpha\, c/d)^{-n}$.

It is obvious from Fig. 3 that for $\sigma_\beta^* > 2\sigma_c$ (curves 3 and 4) the stress intensity factor does exceed the critical stress intensity factor at values of $c/d < 0.05$ and the assumption that $\alpha\, c/d < 1$ is quite justified. Integration of Equation 13 leads to

$$\tau = \frac{1}{A(\sigma_\beta^* - \sigma_c)^n (\pi)^{n/2}} \left[-\frac{2c^{2-n/2}}{(n-2)} M(x)\right]_{c_i}^{c_f} \tag{14}$$

where

$$x = \frac{c}{d},$$

and

$$M(x) = 1 - (n-2)\left[\frac{n\alpha x}{(n-4)} - \cdots\cdots - \frac{n(n+1)(n+2)(n+3)(n+4)}{(n-14)\,6!} (n+5)\alpha^6 x^6\right] \tag{15}$$

If n, the stress corrosion index, is large and initial stress intensity factor $K < 0.9\ K_{Ic}$ (the critical stress intensity factor), the time to failure τ is dominated by the initial flaw size c_i (Beaumont

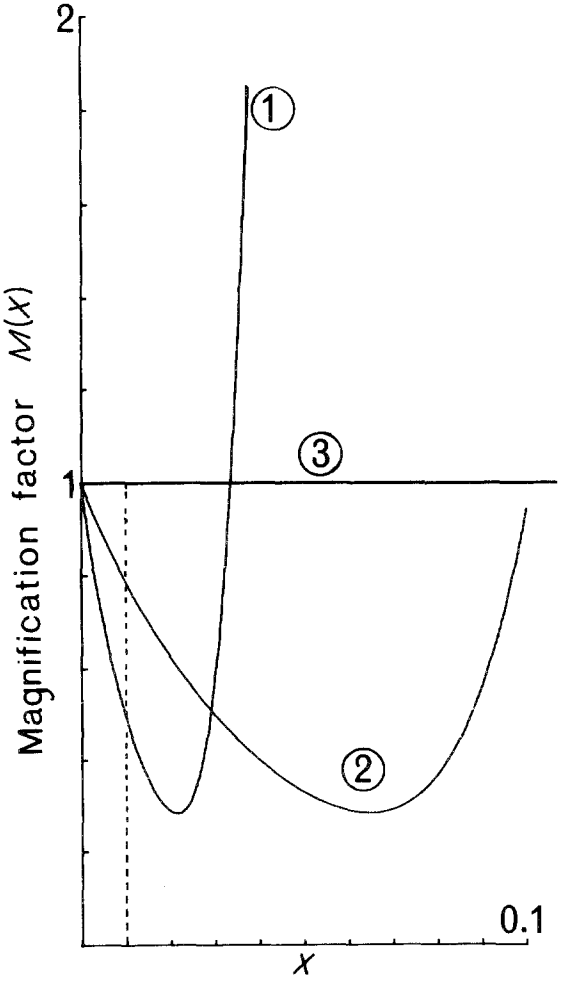

Figure 4 Magnification factor $M(x)$ as a function of the normalized crack length for soda lime glass, where n, the stress corrosion index is 16, for the ratios of applied stress σ_β^* to residual stress σ_c of $\sigma_\beta^*/\sigma_c = 1.5$ (curve 1, 2 (curve 2), 3 (curve 3).

and Young [9], and Equation 14 reduces to

$$\tau = \frac{2M(x_i)c_i^{(2-n)/2}}{A(\sigma_\beta^* - \sigma_c)^n(\pi)^{n/2}(n-2)} \quad (16a)$$

The dimensionless factor $M(x_i)$ may be regarded as a modifying term or magnification factor to the applied stress and becomes increasingly important as $x \to 0.1$.

The variation of the modifying factor $M(x_i)$ with c/d (< 0.1) for values of σ_β^*/σ_c (which determines α) $\leqslant 3$ is shown in Fig. 4 for soda lime glass which has a stress corrosion index of 16. The oscillation in $M(x_i)$ at low values of σ_β^*/σ_c is thought to arise from the limited number of terms chosen* for the plot of $M(x_i)$. For most practical situations (with un-notched specimens) the ratio c/d (typically $c < 20\,\mu$m and $d > 3$ mm) is very small ($< 1\%$). Hence, the region of interest in the plot of $M(x_i)$ in Fig. 4 is the narrow zone of $0 < c/d < 0.01$ where $M(x_i)$ decreases with increasing values of the normalized crack length.

It is now possible to rewrite Equation 16a in a simplified form, as

$$\tau(\sigma_\beta^* - \sigma_c)^n = \text{constant} \quad (16b)$$

Similarly it can be shown that for the dynamic test, the modified expression relating the fracture stress σ_β^* and the stress rate for either chemically or thermally toughened specimens is

$$(\sigma_\beta^* - \sigma_c)^{n+1} = \gamma\dot{\sigma} \quad (17)$$

where σ_c is the value of the residual stress in the outer fibre, $\dot{\sigma}$ is the stressing rate and γ is a constant incorporating the crack propagation constants A, n and the ratio of failure stress σ_c and K_{Ic} (see Evans and Wiederhorn [10]).

4. Discussion

It has been shown that all the equations derived by Evans and co-workers for untoughened will hold for toughened materials, if proper corrections are made for the residual compressive stresses. Although the high tensile stress in the central region does not allow stable crack propagation studies to characterize the corrosion properties, one could still obtain the stress corrosion data fairly quickly from either time failure or dynamic fatigue data.

Analysis of Kirchner and Walker's [1] data of the time to failure for toughened and untoughened alumina shows that the stress corrosion index for untreated alumina in water is 34. For thermally toughened alumina in water, the stress corrosion index is 70, which is anomalously high. When the fracture stresses are corrected, for the toughening residual stresses, one obtains a value of ~ 35. These values compare with the value of 31 obtained by Evans [11].

We have similarly obtained the stress corrosion index of 12 from time to failure data on "1020" toughened soda lime glass. Allowing for the rather limited number of data points and the uncertainty in the value of the residual compressive stress, the value of $n \sim 12$ is in reasonable agreement with values of 14.1 and 16 obtained by Evans [11] and Wiederhorn and Bolz [12] for soda lime glass in water.

Ritter and Cavanagh [13] have recently reported studies on the fatigue resistance of surface recrystallized lithium alumino silicate. By correcting for the residual stresses in the as-drawn specimens, they have obtained excellent agreement in the stress corrosion index for the as-drawn and annealed specimens.

In conclusion, it is interesting to note that the observation by Kirchner and Walker, that the absolute decrease in strength of toughened alumina was slightly greater than that of the untoughened alumina, could be explained on the basis of this analysis. The slightly greater strength degradation for toughened structures is thought to arise from the decrease in the magnification factor M in Equation 16a, as the crack length increases.

It can be seen from Fig. 4 that for the ratio $\sigma_\beta^*/\sigma_c < 3$ (curve 1), there is a reduction in the magnification factor. Because of the initial assumption that n is large and $K_I < 0.9\,K_{Ic}$, fracture will occur at very small values of x_i (the normalized crack length) less than 1% and the reduction in $M(x_i)$ is insignificant. For lower vlaues of the initial bending stress and longer initial flaw sizes the reduction in τ could become more significant.

It is importnat to note that if the applied stress is not high enough to cause failure in a short time, the fact that the crack propagates into an increasingly tensile stress field, will cause an appreciable reduction in the failure time.

*However when the number of terms in the expansion of $M(x)$ equals $n/2$ a singularity occurs.

Acknowledgments

This work was supported by the SRC and the Procurement Executive, Ministry of Defence. The receipt of a preprint by B. R. Lawn and D. B. Marshall in the early stages of this work is gratefully acknowledged. We are grateful also to C. Guillemet for his comments on the paper.

References

1. H. P. KIRCHNER and R. E. WALKER, *Mater. Sic. Eng.* 8 (1971) 301.
2. J. T. HAGAN and M. V. SWAIN, unpublished work (1976).
3. A. G. EVANS and H. JOHNSON, *J. Mater. Sci.* **10** (1975) 214.
4. A. L. ZIJLSTRA and A. J. BURGGRAAF, *J. Non Cryst. Solids* **1** (1968) 49.
5. A. K. VARSHNEYA and R. J. PETTI, *J. Amer. Ceram. Soc.* **59** (1976) 42.
6. B. R. LAWN and D. B. MARSHALL, *Phys. Chem. Glasses* **18** (1977) 1.
7. P. C. PARIS and G. C. SIH, ASTM Special Technical Publication **381** (1965) 30.
8. W. F. BROWN Jr, and J. E. SRAWLEY, ASTM Special Technical Publication **410** (1966) 13.
9. P. W. R. BEAUMONT and R. J. YOUNG, *J. Mater. Sci.* **10** (1975) 1334.
10. A. G. EVANS and S. M. WIEDERHORN, *ibid* 9 (1974) 270.
11. A. G. EVANS, *ibid* 7 (1972) 1137.
12. S. M. WIEDERHORN and H. H. BOLZ, *J. Amer. Ceram. Soc.* **59** (1976) 42.
13. J. E. RITTER Jr and M. S. CAVANAGH, *ibid* **59** (1976) 57.

Received 20 April and 20 May 1977.